Talanta 80 (2010) 1094–1101

Contents lists available at ScienceDirect

Talanta

journal homepage: www.elsevier.com/locate/talanta

Poly(malachite green) at nafion doped multi-walled carbon nanotube composite film for simple aliphatic alcohols sensor

Yogeswaran Umasankar, Arun Prakash Periasamy, Shen-Ming Chen*

Department of Chemical Engineering and Biotechnology, National Taipei University of Technology, No. 1, Section 3, Chung-Hsiao East Road, Taipei 106, Taiwan, ROC

ARTICLE INFO

Article history:
Received 20 May 2009
Received in revised form 15 August 2009
Accepted 24 August 2009
Available online 31 August 2009

Keywords:
Multiwall carbon nanotubes
Malachite green
Composite film
Modified electrodes
Electrocatalysis
Methanol
Ethanol
Propanol

ABSTRACT

Conductive composite film which contains nafion (NF) doped multi-walled carbon nanotubes (MWCNTs) along with the incorporation of poly(malachite green) (PMG) has been synthesized on glassy carbon electrode (GCE), gold and indium tin oxide (ITO) electrodes by potentiostatic methods. The presence of MWCNTs in the composite film (MWCNTs–NF–PMG) enhances surface coverage concentration (Γ) of PMG to ≈396%, and increases the electron transfer rate constant (k_s) to ≈305%. Similarly, electrochemical quartz crystal microbalance study reveals the enhancement in the deposition of PMG at MWCNTs-NF film. The surface morphology of the composite film deposited on ITO electrode has been studied using scanning electron microscopy (SEM) and scanning tunneling microscopy (STM). These two techniques reveal that the PMG incorporated on MWCNTs–NF film. The MWCNTs–NF–PMG composite film also exhibits promising enhanced electrocatalytic activity towards the simple aliphatic alcohols such as methanol, ethanol and propanol. The electroanalytical responses of analytes at NF–PMG and MWCNTs–NF–PMG films were measured using both cyclic voltammetry (CV) and differential pulse voltammetry (DPV). From electroanalytical studies, well defined voltammetric peaks have been obtained at MWCNTs–NF–PMG composite film for methanol, ethanol and propanol at Epa = 609, 614 and 602 mV respectively. The sensitivity of MWCNTs–NF–PMG composite film towards methanol, ethanol and propanol in CV technique are 0.59, 0.36 and 0.92 $\mu A\,mM^{-1}\,cm^{-2}$ respectively, which are higher than NF–PMG film. Further, the sensitivity values obtained using DPV are higher than the values obtained using CV technique.

1. Introduction

Electropolymerization is a simple but powerful method in targeting selective modification of different type electrodes with desired matrices. However, the materials on the matrices do not possess peculiar properties when compared with those materials which are chemically synthesized by traditional methods. The electroactive polymers and carbon nanotubes (CNTs) matrices have received considerable attraction in recent years. Numerous conjugated polymers have been electrochemically synthesized for their application in the fabrication of chemical and biochemical sensor devices [1–3]. These conjugated polymers for sensor devices exhibit interesting enhancement in the electrocatalytic activity towards the oxidation or reduction of several biochemical and inorganic compounds [4] where, some of the functional groups in polymers will act as catalyst [5–7]. In this article, the word "enhanced electrocatalytic activity" could be explained as both; increase in peak current and lower overpotential [8]. The wide variety of applications of matrices made of CNTs for the detection of inorganic and bioorganic compounds such as IO_3^-, ascorbic acid, etc., have already been reported in the literature [9–12].

Even though the electrocatalytic activity of conjugated polymers and CNTs matrices individually shows good results; some properties like mechanical stability, sensitivity for different techniques, and electrocatalysis for multiple compound detections are found to be poor. To overcome this difficulty, new studies have been developed in the past decade for the preparation of composite films composed of both CNTs and conjugated polymers. The rolled-up graphene sheets of carbon exhibit π-conjugative structure with highly hydrophobic surface. This unique property of the CNTs allows them to interact with organic aromatic compounds through π–π electronic and hydrophobic interactions to form new structures [13,14]. There were past attempts in the preparation of composite and sandwiched films made of polymer adsorbed on CNTs, and used them for electrocatalytic studies such as, selective detection of dopamine in the presence of ascorbic acid [15]. The sandwiched films were also been used in the designing of nanodevices with the help of noncovalent adsorption, electrodeposition, etc. [16].

Among these conjugated polymers, a group of them representing azines such as phenazines, phenothiazines, phenoxazines, etc., have a wide use in bioelectrochemistry as redox indica-

* Corresponding author. Tel.: +886 2270 17147; fax: +886 2270 25238.
E-mail address: smchen78@ms15.hinet.net (S.-M. Chen).

0039-9140/$ – see front matter © 2009 Elsevier B.V. All rights reserved.
doi:10.1016/j.talanta.2009.08.034

tors and mediators [17]. The electropolymerization of azine group compounds are usually performed by anodic oxidation in acidic medium [18,19]. Similar to these azine dyes, malachite green (MG) is also a dye compound which has an open but ionized structure, and hence the resulting polymer is promising in exhibiting interesting features like fast rate of charge transfer and ion transport and nice catalytic ability towards small bio-molecules [20]. Previous studies reported poly(malachite green) (PMG) can be synthesized by electrochemical polymerization of malachite green. These studies also reported the growth mechanism of PMG along with the electrochemical, FT-IR and UV–vis studies [20,21]. The chemical structures of MG and PMG are given in Scheme 1.

The oxidation of simple aliphatic alcohols to the corresponding products is an important transformation in organic synthesis. Recently, from the environmental point of view, various catalytic methods using oxidants have been reported [22–25]. Among these, methanol has been widely used in the direct methanol fuel cells at lower temperatures, where the methanol oxidation was done with the help of metal oxide catalysts [26,27]. Similarly, ethanol is the most common substance consumed by humans and it is frequently a contributory factor in a variety of accidents. Further, the determination of ethanol is very important to control the fermentation processes in some industrial fields, which includes the pulp, food and beverage industries. The measurement of ethanol is particularly needed for quality control of beer, wines and spirits [28–30]. The oxidation of propanol is also an important transformation in laboratory and industrial synthetic chemistry, which could be used as important intermediate for the synthesis of chemicals [31]. Various methods have been reported for the determination of simple aliphatic alcohols with the help of different techniques [28,32]. Within these several methods of determination, the electrochemical methods have more advantages over the others in sensing the analytes [33–35].

The literature survey reveals that there were no previous attempts made for the synthesis of composite film composed of CNTs, nafion (NF) and PMG for the use in sensor application. In this article, we report a novel composite film made of multi-walled carbon nanotubes (MWCNTs) which have been dispersed in NF, and incorporated with PMG. MWCNTs–NF–PMG composite film's characterization, enhancement in functional properties, peak current and electrocatalytic activity have also been reported along with its application in the determination of methanol, ethanol and propanol. The film formation processing involves the modification of electrodes with uniformly well dispersed MWCNTs–NF, and which is then modified with PMG.

2. Experimental

2.1. Materials

PMG, NF, MWCNTs (OD = 10–20 nm, ID = 2–10 nm and length = 0.5–200 μm), methanol, ethanol and propanol obtained from Aldrich and Sigma–Aldrich were used as received. All other chemicals used were of analytical grade. The preparation of aqueous solution was done with twice distilled deionized water. Solutions were deoxygenated by purging with pre-purified nitrogen gas. The pH 1.0 aqueous solution was prepared from H_2SO_4. The pH 4.0 aqueous solution was prepared from 0.01 M potassium hydrogen phthalate (KHP) solution, which was then added to 0.1 M Na_2SO_4 solution (1:1).

2.2. Apparatus

Cyclic voltammetry (CV), electrochemical quartz crystal microbalance (EQCM) and differential pulse voltammetry (DPV)

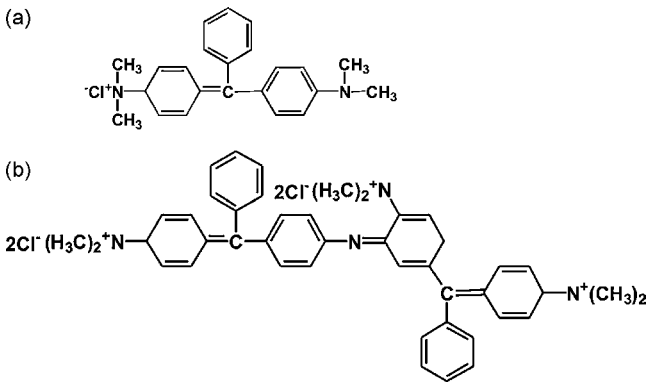

Scheme 1. Chemical structure of MG and PMG.

were performed using analytical system models CHI-405, CHI-400 and CHI-750 potentiostats respectively. A conventional three-electrode cell assembly consisting of an Ag/AgCl reference electrode and a Pt wire counter electrode were used for the electrochemical measurements. The working electrode was glassy carbon electrode (GCE) modified with PMG, NF, NF–PMG or MWCNT–NF–PMG composite films. In these experiments, all the potentials are reported vs. Ag/AgCl reference electrode. The working electrode for EQCM measurements was an 8 MHz AT-cut quartz crystal coated with a gold electrode. The diameter of the quartz crystal is 13.7 mm; the gold electrode diameter is 5 mm. The morphological characterizations of the films were examined by means of scanning electron microscopy (SEM) (Hitachi S-3000H) and scanning tunneling microscopy (STM) (Being Nano-Instruments CSPM4000). All the measurements were carried out at 25 ± 2 °C.

2.3. Preparation of MWCNT–NF–PMG composite electrodes

The important challenge in the preparation of MWCNTs was the difficulty in dispersing them in to a homogeneous solution. Generally, the dispersion of CNTs has been carried out by physical (milling) and chemical methods (covalent and noncovalent functionalization). These methods cause damage to CNTs and add impurities to it [36,37]. To overcome these drawbacks, hydrophobic interaction between NF and MWCNTs has been used for our experiments [38,39]. Briefly, 5% NF prepared by adding 2 ml of NF in 10 ml water, which was used to disperse 10 mg of MWCNTs. The uniform dispersion of MWCNTs was obtained by 6 h ultrasonication of MWCNTs–NF mixture.

Before starting each experiment, GCEs were polished by BAS polishing kit with 0.05 μm alumina slurry, then rinsed and then ultrasonicated in double distilled deionized water. The GCEs studied were uniformly coated with 10 μl of MWCNTs–NF mixture (0.13 mg cm^{-2} of MWCNTs) and dried at room temperature. Then, MG (0.5 mM) was electropolymerized on the MWCNT–NF modified GCE, which was present in pH 4 KHP aqueous solution. The electropolymerization was performed by consecutive CVs over a suitable potential range of −0.3 to 1.4 V. Then, the modified MWCNT–NF–PMG electrode was carefully washed with double distilled deionized water. The concentrations of homogeneously dispersed MWCNTs–NF were exactly measured using micro-syringe.

3. Results and discussions

3.1. Electropolymerization of PMG at MWCNTs–NF composite film

The electropolymerization of MG (0.5 mM) using electrochemical oxidation on unmodified, MWCNT–NF modified, and only

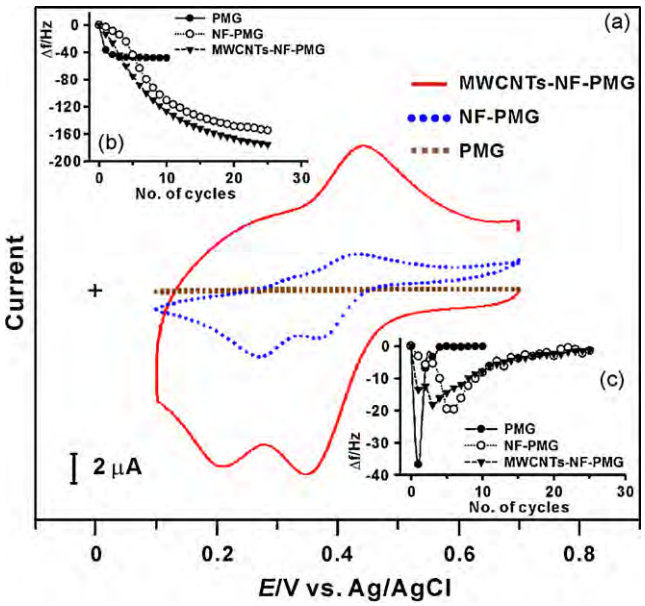

Fig. 1. (a) CVs of GCE modified from PMG, NF–PMG and MWCNTs–NF–PMG films in KHP solution, scan rate at 20 mV s^{-1}. EQCM frequency change responses recorded together with consecutive CVs (PMG formation on NF, MWCNTs–NF modified and unmodified gold electrodes, potential between −0.2 and 1.4 V; scan rate: 100 mV s^{-1}), where (b) shows the gross change in the frequency shift vs. scan cycles, whereas (c) shows the change between each consecutive scans.

NF modified GCEs have been performed for the preparation and comparative studies of PMG, NF–PMG and MWCNT–NF–PMG composite films. On subsequent cycles, the redox peaks corresponding to PMG have found growing in all these films (figures not shown). This above result indicates that during the cycles, deposition of PMG takes place on the electrode surface. However, there are no peaks representing PMG appears at bare GCE. The optimized number of cycles for the deposition of PMG at MWCNTs–NF modified GCE using CV technique is 25. This optimization is done by observing the monomer oxidation current at Epa = 0.99 V, where the Ipa decreases during cycling and the oxidation peak disappears after 25 cycles. These above prepared three films (PMG, NF–PMG and MWCNT–NF–PMG) have been characterized using various electrochemical techniques in pH 4.0 KHP or pH 1.0 aqueous solution. Before transferring the films in to aqueous solution for other electrochemical characterizations, the prepared films have been washed carefully in deionized water to remove the loosely attached non-polymerized MG monomer on the modified GCE. Fig. 1(a) shows the reversible and irreversible redox couples of PMG, NF–PMG and MWCNT–NF–PMG modified GCEs. The corresponding CVs have been measured at 20 mV s^{-1} scan rate in the potential range of 0.7–0.1 V. Among these three films, the $E^{0\prime}$ values of both redox couples for MWCNT–NF–PMG composite film are at 395 mV (Redox-I) and 210 mV (Redox-II) vs. Ag/AgCl in KHP aqueous solution. Among these two redox couples, the $E^{0\prime}$ at 395 mV is the redox reaction of PMG and $E^{0\prime}$ at 395 mV could be the redox reaction of MG's dimer. The Epa, Epc and Ipc values of PMG at various film modified electrodes are given in Table 1. Interestingly the values in Table 1 reveal, MWCNT-NF modified GCE has higher polymerizing current for PMG than at other modified or unmodified GCEs. Further, the presence of MWCNTs in the MWCNT–NF–PMG composite film increases the overall back ground current. These above results represent more deposition of PMG on MWCNT-NF modified GCE than on other GCEs.

Table 2
Surface coverage concentration (Γ) of various species present in PMG at different modified electrodes obtained using CV studies.

Modified electrode	Type of film	Γ (pmol cm^{-2})	
		Redox-I	Redox-II
GCE	[a]-PMG	490	145
	[b]-PMG	2430	177
Gold	[a]-PMG	139	20.5
	[b]-PMG	229	115
ITO	[b]-PMG	675	–

[a] PMG electropolymerized on NF modified electrode.
[b] PMG electropolymerized on MWCNTs–NF modified electrode.

The increase in deposition of PMG in the presence of MWCNTs is evident with the active surface coverage concentration (Γ) given in Table 2 where, Γ of both species (Redox-I and -II) of PMG enhances at MWCNTs-NF film modified GCE when comparing at only NF and bare GCE. The calculated values from the same table shows that, MWCNTs enhances Γ of PMG by 15 pmol cm^{-2} μg^{-1}; and the overall increase in percentage of PMG Γ at MWCNTs film is 396%. In these Γ calculations, the number of electrons involved in PMG redox reactions is assumed as two. The comparison of PMG, NF–PMG and MWCNT–NF–PMG films on gold and indium tin oxide (ITO) electrodes are given in supplementary materials, which show that MWCNTs catalyze the PMG electropolymerization similar in that of GCE. However, the comparison of Epa and Epc values in Table 1 shows that the Redox-I of MWCNT–NF–PMG composite film at GCE and gold electrode is highly reversible than at ITO electrode, where ΔE at GCE and gold electrode is 93.2 mV and ITO electrode is 198 mV vs. Ag/AgCl. In these above experiments too, MWCNT-NF modified electrodes show higher polymerizing current for PMG than at other modified or unmodified electrodes, which are consistent with the Ipc and Γ values given in Tables 1 and 2, respectively. The possible interactions between MWCNTs, NF and PMG present in the composite film are given in Scheme 2, where the interaction between MWCNTs and NF is hydrophobic, and the interaction between NF and PMG is both hydrophobic and electrostatic interactions.

The MG electropolymerization is further confirmed using EQCM experiments, which have been carried out by modifying the gold in electrochemical quartz crystal with uniformly coated MWCNTs-NF or NF and then dried at 40 °C. The increase in voltammetric peak

Table 1
Epa, Epc and Ipc values of redox reactions of PMG at various modified electrodes present in pH 4.0 KHP aqueous solution.

Modified Electrodes		Epa (mV)	Epc (mV)		Ipc (μA)	
Electrodes	Films	Redox-I	Redox-I	Redox-II	Redox-I	Redox-II
GCE	[a]-PMG	434.5	366.9	270.8	−3.33	−1.41
	[b]-PMG	441.4	348.2	210.0	−10.42	−1.53
Gold	[a]-PMG	453.1	332.6	234.5	−0.53	−0.09
	[b]-PMG	441.4	348.2	214.9	−2.83	−0.33
ITO	[b]-PMG	433.5	235.5	–	−11.64	–

[a] PMG electropolymerized on NF modified electrode.
[b] PMG electropolymerized on MWCNTs–NF modified electrode.

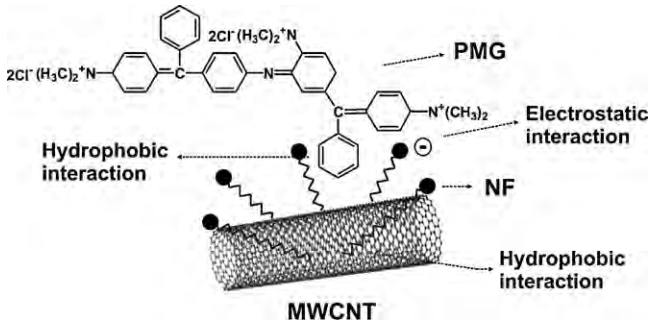

Scheme 2. Possible interactions between MWCNTs, NF and PMG present in MWCNTs–NF–PMG composite film.

current of PMG redox couple and the frequency decrease (or mass increase) are found to be consistent with the growth of PMG film on MWCNTs-NF or NF modified gold electrode (figures not shown). These results too show that the obvious deposition potential has started between −0.2 and 1.4 V. From the frequency change, the change in the mass of composite film at the quartz crystal can be calculated by the Sauerbrey equation (1), however 1 Hz frequency change is equivalent to 1.4 ng cm^{-2} of mass change [40,41]. The mass change during PMG incorporation on MWCNTs-NF modified, NF modified and unmodified gold electrodes for total cycles are 246, 217 and 68 ng cm^{-2} respectively.

$$\text{Mass change } (\Delta m) = -\tfrac{1}{2}(f_0^{-2})(\Delta f)A(K\rho)^{1/2} \quad (1)$$

where f_0 is the oscillation frequency of the crystal; Δf is the frequency change; A, the area of gold disk; K, the shear modulus of the crystal; ρ, the density of the crystal. Fig. 1(b) indicates the variation of frequency with increase of scan cycles for PMG at bare gold electrode, NF modified and MWCNTs–NF modified gold electrodes. Fig. 1(c) indicates every cycle of frequency with the increase of scan cycles for PMG at bare gold electrode, NF modified and MWCNTs–NF modified gold electrodes. These EQCM results prove that the deposition of PMG on the MWCNTs-NF film is more stabilized and more homogeneous than on the NF modified or bare gold electrodes.

3.2. Surface morphological studies of MWCNTs–NF, NF–PMG and MWCNTs–NF–PMG composite films

Three different films MWCNTs–NF, NF–PMG and MWCNTs–NF–PMG have been prepared on ITO electrodes with similar conditions and similar potential as that of GCE, and were characterized using SEM. Comparison of Fig. 2(a–c) reveals significant morphological difference between all the three films. The top views of nanostructures in Fig. 2(a) on the ITO electrode surface show uniformly deposited homogeneously dispersed MWCNTs in NF. The NF–PMG film in Fig. 2(b) shows elongated beads of NF and PMG deposited over ITO electrode surface. However, there are no bead formations if only NF coated over ITO, instead a porous NF film is formed (image not shown). Similarly, a uniform thin film with no morphology is formed for only PMG deposited over ITO electrode surface. The MWCNTs–NF–PMG composite film in Fig. 2(c) shows that plateaus of PMG formed over MWCNTs–NF film. Further, in Fig. 2(c) MWCNTs are not obviously visible as in Fig. 2(a), because PMG deposition covered over MWCNTs. These results in Fig. 2(c) could be explained as the increase in deposition of PMG over MWCNTs–NF, which creates plateaus instead of beads and covers over MWCNTs. The same three film modified ITO electrodes have been used to measure STM topography images shown in Fig. 3(a–c). The higher magnification (7 μm × 7 μm) of STM images than that of SEM images reveals that in Fig. 3(a)

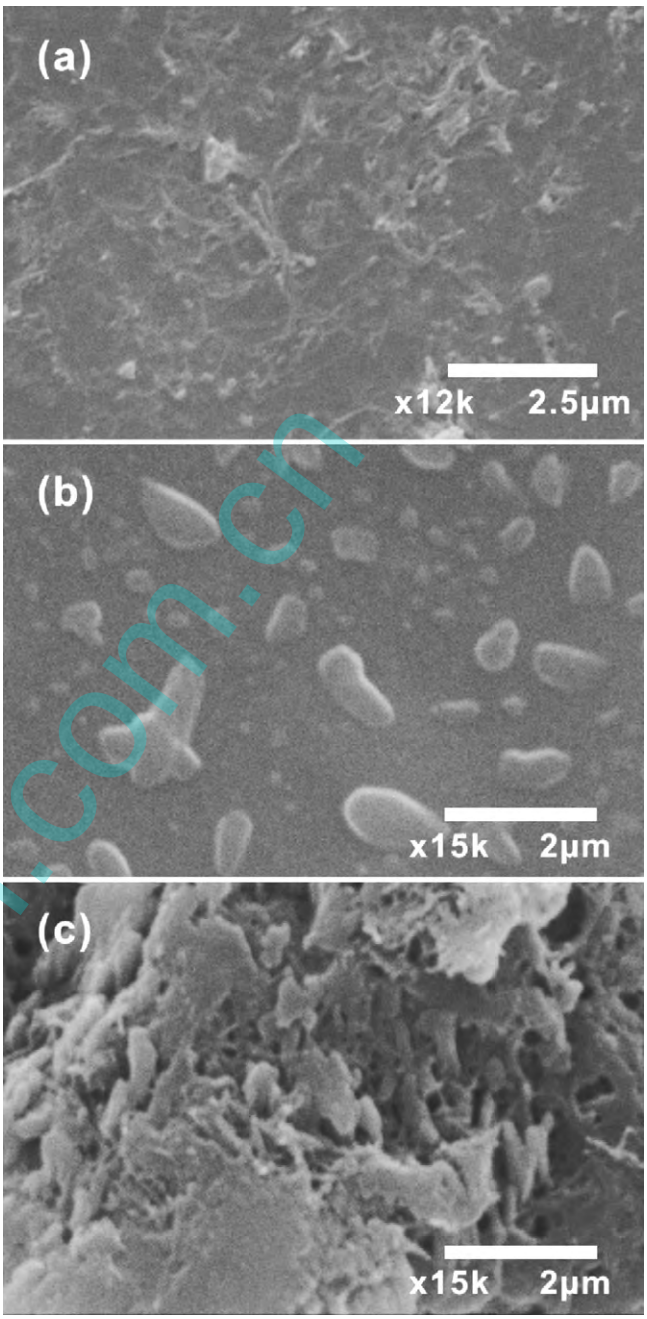

Fig. 2. SEM images of (a) MWCNTs–NF, (b) NF–PMG and (c) MWCNTs–NF–PMG films.

well dispersed MWCNTs in NF coated over ITO electrode. Similarly in Fig. 3(b), formation of nanometer sized grains in between PMG beads and in Fig. 3(c) more deposition of PMG over MWCNTs. These above details are not clearly visible in SEM images. Comparison of Fig. 3(a) with Fig. 3(c) also reveals that higher concentration of PMG deposited on MWCNTs modified ITO electrode, which is consistent with the Γ values shown in Table 2. Further, the thicknesses of MWCNTs–NF, NF–PMG and MWCNTs–NF–PMG obtained using STM results are 120, 70 and 180 nm respectively. These values too show MWCNTs–NF–PMG has higher thickness than the other two films, which is due to the presence of MWCNTs–NF covered under PMG film. These SEM and STM results reveal the coexistence of MWCNTs–NF and PMG in the composite film.

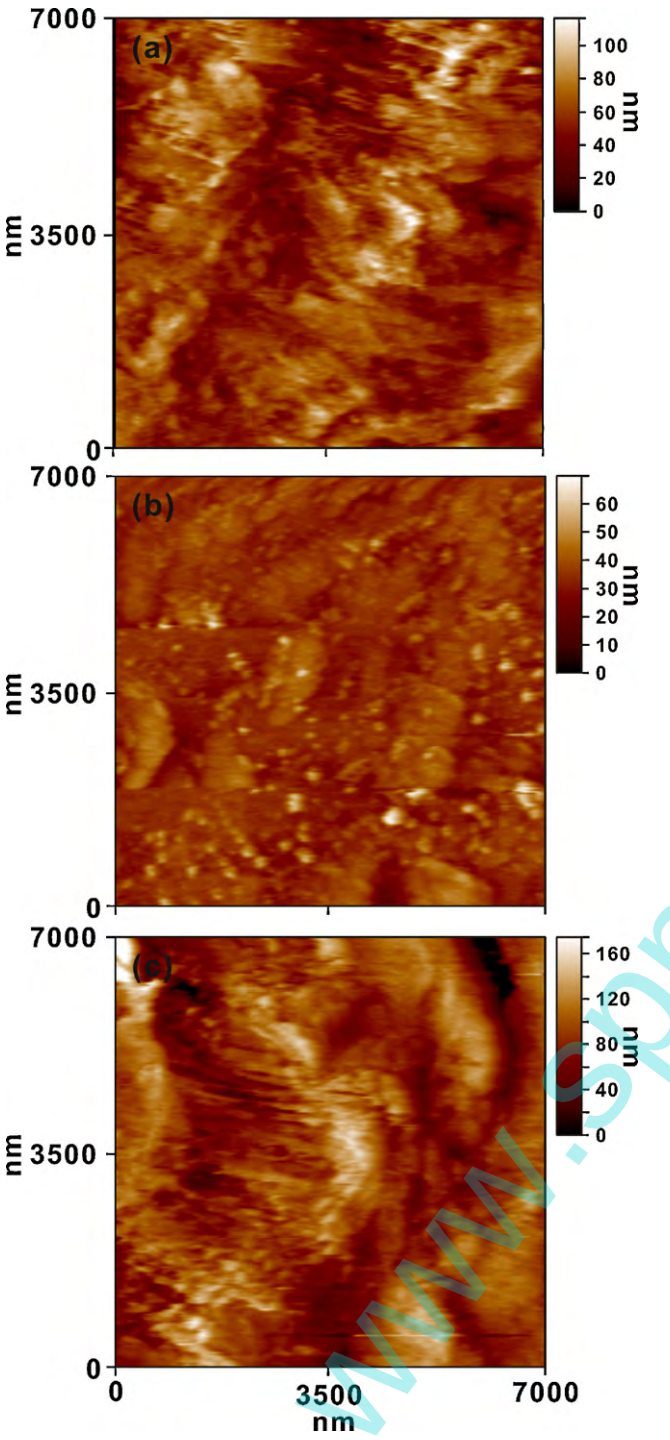

Fig. 3. STM images of (a) MWCNTs–NF, (b) NF–PMG and (c) MWCNTs–NF–PMG films.

3.3. Electrochemical and stability studies of MWCNTs–NF–PMG composite film

The CVs of NF–PMG and MWCNTs–NF–PMG composite films on GCE in pH 4.0 KHP aqueous solution at different scan rates show that the anodic and cathodic peak currents of the composite film's redox couple, which increases linearly with the increase of scan rates (figure not shown). The ratio of Ipa/Ipc for both the film demonstrates that the redox process is not controlled by diffusion. However, the ΔEp of each scan rate reveals that the peak separation of both film's redox couple increases as the scan rate increase. From the slope values of ΔE vs. log scan rate, by assuming the value of $\alpha \approx 0.5$, number of electrons involved as two, the electron transfer rate constant (k_s) has been calculated using Eq. (2) based on Laviron theory [42].

$$\log k_s = \alpha \log(1-\alpha) + (1-\alpha)\log \alpha - \log\left(\frac{RT}{nF\upsilon}\right) - \alpha(1-\alpha)nF\frac{\Delta E}{2.3RT} \quad (2)$$

In Eq. (2), the scan rate and ΔE values are in unit volts. The k_s values obtained are 0.12 and 0.49 s^{-1} for NF–PMG and MWCNTs–NF–PMG modified GCEs respectively. From these k_s values, the increase in ability of electron transfer between the electrode surface and PMG in presence of MWCNTs is ≈305%. The reproducibility of the obtained k_s values for both NF–PMG and MWCNTs–NF–PMG films have also been studied, where the relative standard deviation (RSD) values obtained are 5% ($n = 7$) for NF–PMG and 7% ($n = 7$) for MWCNTs–NF–PMG films. These results show the enhancement in functional property of MWCNTs–NF–PMG composite film in the presence of MWCNTs.

Fig. 4(a) shows the CVs of MWCNTs–NF–PMG on GCE obtained in pH 4.0 KHP aqueous solution, then washed with deionized water, and was transferred to various pH aqueous buffer solutions without the presence of MG. The results show that the film is highly stable in the pH range between 1 and 13. The values of Epa and Epc depend on the pH value of buffer solution. The inset in Fig. 4(a) shows the formal potential of MWCNTs–NF–PMG plotted over the pH range from 1 to 13. The response shows a slope of −65 mV pH^{-1}, which is close to that given by Nernstian equation for equal number of electrons and protons transfer. All these above results show the enhancement in functional properties of MWCNTs–NF–PMG composite film due to the presence of both PMG and MWCNTs.

The enhancement in stability of PMG in the presence of MWCNTs has been studied, and the percentage of degradation of MWCNTs–NF–PMG and NF–PMG calculated using an equation given in the previous literature [43]. The experimental results in Fig. 4(b) indicates the successive 280 min cycling (scan rate 20 mV s^{-1}) applied over a potential range of 0.1–0.7 V on MWCNTs–NF–PMG and NF–PMG in pH 4.0 KHP aqueous solution. The CVs have been recorded at the interval of 30 min each; from which the values of Ipc were noted and plotted against time. From these results it is clear that after 220 min the response of MWCNTs–NF–PMG becomes constant with time and cycling, indicating it is a stable film. However, the NF–PMG continues to degrade upon cycling. The amount of degradation after 280 min cycling for MWCNTs–NF–PMG and NF–PMG are 29% and 63% respectively. From this above result, the percentage of decrease in degradation of PMG in presence of MWCNTs is about 34% for 280 min cycling. Similar enhancements in CNTs with polymer composite properties when comparing CNT or polymer alone were already reported in the literature [44]. Repeatability of the stability studies have also been carried out at 280 min cycling for MWCNTs–NF–PMG film, where the RSD value obtained is 6% ($n = 3$).

3.4. Electroanalytical responses of methanol, ethanol and propanol at MWCNTs–NF–PMG composite film

The MWCNTs–NF–PMG composite film has been synthesized on GCE at similar conditions as given in Section 2. Then the composite film modified electrode has been washed carefully in deionized water and transferred to pH 1 aqueous solution for the electrocatalysis studies of methanol, ethanol and propanol. All the CVs have been recorded at the constant time interval of 1 min with nitrogen purging before the start of each experiments. Fig. 5(a–c) shows the electrocatalytic oxidation of methanol, ethanol and propanol

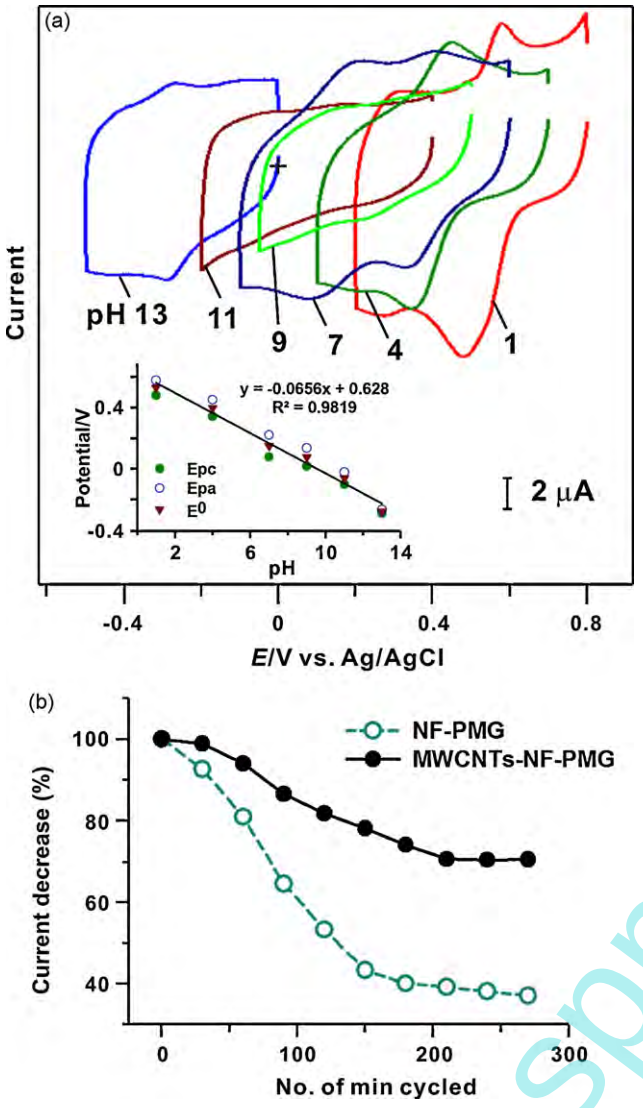

Fig. 4. (a) CVs of the MWCNTs–NF–PMG film synthesized using pH 4.0 KHP solution on GCE and transferred to various pH solutions. The insets shows Epa, Epc and the formal potential vs. pH from 1 to 13 (slope = −65 mV/pH), where the slope is almost nearer to Nernstian equation for equal number of electrons and protons transfer. (b) Number of minutes cycled vs. current decrease in (%) for NF–PMG and MWCNTs–NF–PMG films, which shows that MWCNTs–NF–PMG is highly stable when comparing with NF–PMG.

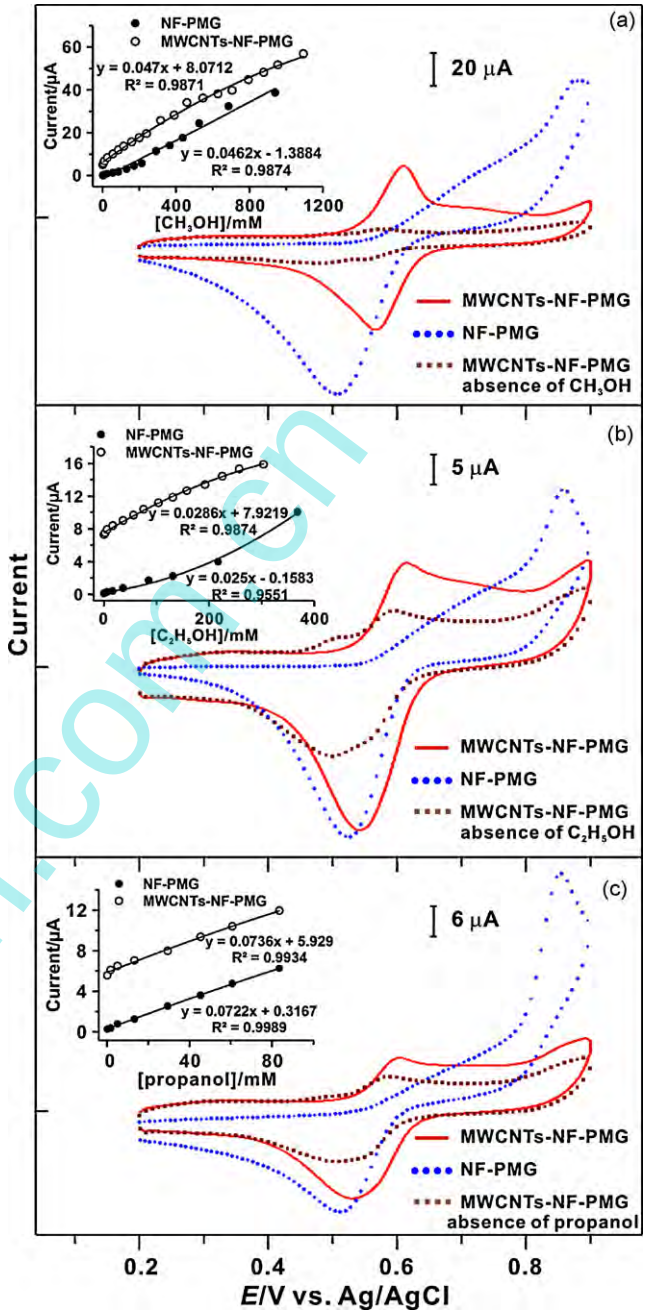

Fig. 5. The CVs in (a) is the comparison of 0 and 0.96 M of methanol at MWCNTs–NF–PMG with that of 0.96 M of methanol at NF–PMG in pH 1 aqueous solution; (b) is the comparison of 0 and 0.3 M of ethanol at MWCNTs–NF–PMG with that of 0.3 M of ethanol at NF–PMG at similar conditions and (c) is the comparison of 0 and 0.08 M of propanol at MWCNTs–NF–PMG with that of 0.08 M of propanol at NF–PMG at similar conditions. The insets in (a–c) show the plot of current vs. different concentration of methanol, ethanol and propanol respectively at MWCNTs–NF–PMG and NF–PMG. In these results, the analytes show higher electrocatalytic activity at MWCNTs–NF–PMG film.

at NF–PMG and MWCNTs–NF–PMG composite films respectively; scan rate 20 mV s^{-1}. In all the sections of Fig. 5, electrocatalytic activity at MWCNTs–NF–PMG composite films are shown with (higher concentration) and without the presence of analytes. However for NF–PMG film, only higher concentrations of analytes are shown, where the highest concentration of analytes are 0.96 M for methanol, 0.3 M for ethanol and 0.08 M for propanol. The CVs for MWCNTs–NF–PMG exhibits respective redox couples as discussed in Section 3.1 in the absence of analytes, and upon addition of analytes, new growth in the oxidation peak of respective analytes appears at Epa = 609, 614 and 602 mV for methanol, ethanol and propanol respectively. These peak currents show that electrocatalytic oxidation of all three analytes takes place at PMG redox couple. The methanol, ethanol and propanol oxidation at MWCNTs–NF–PMG composite film could be given by the following equations.

$$CH_3OH \rightarrow CO_{ads} + 4H^+ + e^- \quad (3)$$

$$C_2H_5OH \rightarrow CH_4 + CO_{ads} + 2H^+ + (1/2)e^- \quad (4)$$

$$(CH_3)_2CHOH \rightarrow C_2H_4 + CO_{ads} + 4H^+ + e^- \quad (5)$$

$$CO_{ads} + H_2O \rightarrow CO_2 + 2H^+ + 2e^- \quad (6)$$

In these above electrocatalysis experiments, an increase in concentration of methanol (3.12 mM) to (1.1 M), ethanol (2.06 mM) to (0.3 M) and propanol (1.65 mM) to (83.4 mM) simultaneously produces a linear increase in the oxidation peak currents of the respective analytes with good film stability at NF–PMG and

MWCNTs–NF–PMG films. The anodic peak currents are linear with the concentration of analytes. It is obvious that MWCNTs–NF–PMG shows higher electrocatalytic activity for the analytes. More specifically, the enhanced electrocatalytic activity of MWCNTs–NF–PMG can be defined in terms of both the lower in overpotential and higher peak current than that of NF–PMG film. These results can be observed from the Ipa and Epa values of various analytes, which are given in supplementary materials. Where, the increase in peak current and decrease in over potential; both are considered as the electrocatalytic activity [8]. The calculated limit of detections (LOD) at NF–PMG is 10.7 mM for methanol, 8 mM for ethanol and 1.8 mM for propanol. Similarly, the LOD at MWCNTs–NF–PMG is 8.3 mM for methanol, 5.1 mM for ethanol and 0.6 mM for propanol.

From the slopes of linear calibration curves, the sensitivities of NF–PMG and MWCNTs–NF–PMG composite film modified GCEs have been calculated. The sensitivity values of NF–PMG are 0.58 $\mu A\,mM^{-1}\,cm^{-2}$ for methanol, 0.31 $\mu A\,mM^{-1}\,cm^{-2}$ for ethanol and 0.90 $\mu A\,mM^{-1}\,cm^{-2}$ for propanol. Similarly, the sensitivity values of MWCNTs–NF–PMG are 0.59 $\mu A\,mM^{-1}\,cm^{-2}$ for methanol, 0.36 $\mu A\,mM^{-1}\,cm^{-2}$ for ethanol and 0.92 $\mu A\,mM^{-1}\,cm^{-2}$ for propanol. The correlation coefficients of linear calibration curves at NF–PMG are 0.9874, 0.9551 and 0.9989 for methanol, ethanol and propanol respectively. Similarly, correlation coefficients obtained at MWCNTs–NF–PMG are 0.9871, 0.9874 and 0.9934 for methanol, ethanol and propanol respectively. It is obvious that the sensitivity of MWCNTs–NF–PMG film is higher for all the three analytes when compared with NF–PMG film. The reproducibility of NF–PMG and MWCNTs–NF–PMG films on GCE has also been studied for all the three analytes using CV technique (36 h; $n = 4$). The results show that there is an enhancement in reproducibility for all the three analytes in presence of MWCNTs at the film. The values are 38% enhancement for methanol, 47% enhancement for ethanol and 62% enhancement for propanol in presence of MWCNTs. The overall view of these results, clearly reveal that MWCNTs–NF–PMG composite film is efficient than NF–PMG film for methanol, ethanol and propanol detection.

3.5. DPV studies of methanol, ethanol and propanol at MWCNTs–NF–PMG composite film

Fig. 6(a–c) shows the DPVs which have been obtained for methanol, ethanol and propanol at MWCNTs–NF–PMG composite film respectively. The DPVs have been recorded at a constant time interval of 1 min with nitrogen purging before the start of each experiment. They demonstrate that the calibration curves for the three analytes are linear for a wide range of concentrations; for methanol from 1.55 to 95.44 mM, ethanol from 3.09 to 72.48 mM and for propanol from 6.12 to 48.98 mM. The calculated LODs are 0.6 mM for methanol, 0.1 mM for ethanol and 6.9 mM for propanol. Similarly, the limit of quantifications (LOQ) is 2 mM for methanol, 0.4 mM for ethanol and 21.1 mM for propanol. From the slopes of linear calibration curves, the sensitivity of MWCNTs–NF–PMG composite film modified GCE towards all three analytes have been calculated. The sensitivity values are 19.62 $\mu A\,mM^{-1}\,cm^{-2}$ for methanol, 3.75 $\mu A\,mM^{-1}\,cm^{-2}$ for ethanol and 4.06 $\mu A\,mM^{-1}\,cm^{-2}$ for propanol. The correlation coefficients of linear calibration curves are 0.9786, 0.9933 and 0.9988 for methanol, ethanol and propanol respectively. When comparing these sensitivity values with the values obtained in CV studies reveals that DPV technique possess higher sensitivity than CV technique. These results show that DPV technique is more efficient than CV technique for methanol, ethanol and propanol detection at MWCNTs–NF–PMG composite film.

The interference of ascorbic acid (AA) and uric acid (UA) during methanol determination has been studied using DPV technique. In these experiments, methanol concentration has been kept constant

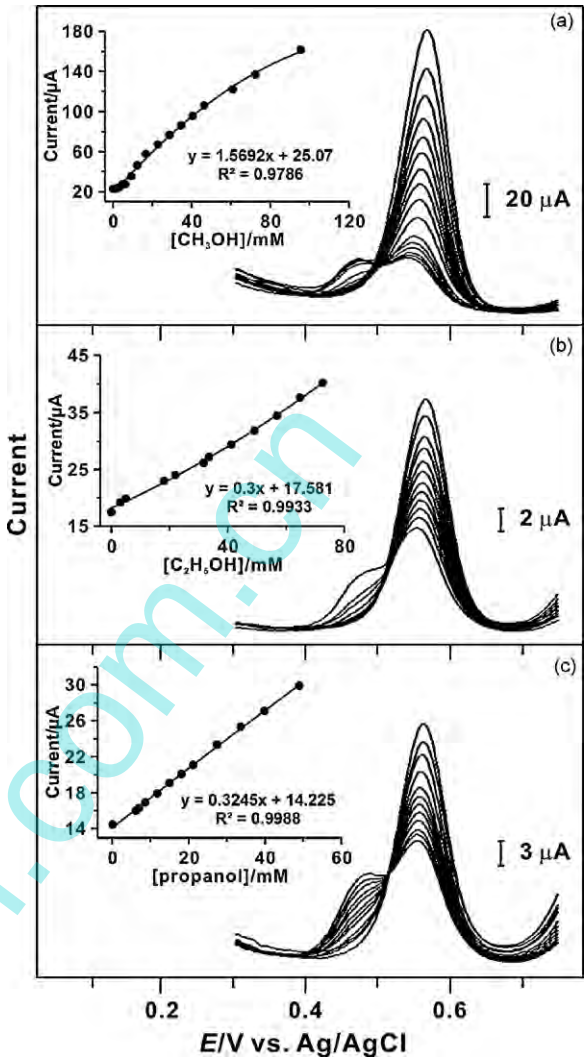

Fig. 6. DPVs of MWCNTs–NF–PMG film shown in (a) various concentrations of methanol (0.0; 1.55–95.44 mM); (b) various concentrations of ethanol (0.0; 3.09–72.48 mM) and (c) various concentrations of propanol (0.0; 6.12–48.98 mM) in pH 1 aqueous solution. The insets in (a–c) show the plot of current vs. different concentration of methanol, ethanol and propanol at MWCNTs–NF–PMG film respectively.

(2.3 mM) and the concentrations of AA and UA have been increased from 24.9 μM to 0.9 mM. The results reveal that there is no obvious change in the methanols' peak current during the addition of AA and UA. The change in peak current of methanol during the addition of AA is 2% with RSD = 1% ($n = 6$), whereas for UA it is 5% with RSD <1% ($n = 6$). Similarly, the interference of glycerin during ethanol determination has also been studied, where the ethanol concentration kept at 2.6 mM, and the concentration change of glycerin is from 1.3 to 87.2 mM. Results show that the change in ethanol peak current during the addition of glycerin is 9% with RSD = 2% ($n = 6$). The above data reveal that MWCNTs–NF–PMG composite film could be used for the efficient determination of simple aliphatic alcohols.

3.6. Analysis of methanol, ethanol and propanol containing real samples

The performance of MWCNTs–NF–PMG composite film modified GCE has been tested by applying it to the determination of the analytes present in real samples. The technique used for the determination was DPV. In these experiments, the real sample of methanol is green (scar removal and ache treatment agent),

Table 3
Electroanalytical results of simple aliphatic alcohol determination present in real samples using DPV in pH 1.0 aqueous solution at MWCNTs–NF–PMG composite film modified GCE.

Sample	Added (mM)	Found (mM)	Recovery (%)	RSD (%)	LOQ (mM)
Methanol (scar removal and ache treatment agent)	3.10	2.94	94.5	3	8.6
	4.64	4.74	102.1		
	9.23	9.00	97.4		
Ethanol (white wine)	0.56	0.58	97.0	2	8.3
	9.73	9.55	101.8		
	10.77	10.70	100.6		
Propanol (protan tablets)	16.02	15.98	100.2	2	3.5
	24.97	25.05	99.7		
	33.85	32.73	103.3		

ethanol is white wine, and propanol is protan tablets. The scar removal and ache treatment agent's labeled composition is triclosan, hyaluronic acid, collagen, glycerine, catechins, etc., along with methanol as solvent. Similarly, the white wine's labeled composition is 13% ethanol, and the protan tablet's labeled composition is 70% propanol. The scar removal and ache treatment agent was obtained from Stylecosmo International, France. The white wine is the product of Domaine de Pourthce, France, and the protan tablets were obtained from Protan, USA. In these experiments, the concentration added, concentration found, recovery, RSD and LOQ are given in Table 3. These above results show that MWCNTs–NF–PMG composite film is efficient for methanol, ethanol and propanol detection.

4. Conclusions

We developed a novel composite material using MWCNTs, NF and PMG at GCE, gold and ITO electrodes, which are more stable in pH 1–4 aqueous solutions. The developed MWCNTs–NF–PMG composite film for the electrocatalysis combines the advantages of ease of fabrication, high reproducibility and sufficient long-term stability. The EQCM results confirmed the incorporation of PMG on MWCNTs–NF modified gold electrode. The SEM and STM results have shown the difference between MWCNTs–NF, NF–PMG and MWCNTs–NF–PMG composite films morphology. Further, it has been found that MWCNTs–NF–PMG composite film has excellent functional properties along with good electrocatalytic activity towards methanol, ethanol and propanol. The experimental methods of CV and DPV with MWCNTs–NF–PMG composite film sensor integrated into the GCE which is presented in this article provide an opportunity for qualitative and quantitative characterization. Therefore, this work establishes and illustrates in principle and potential, a simple and novel approach for the development of a voltammetric sensor which is based on modified GCE.

Acknowledgements

This work was supported by the National Science Council and the Ministry of Education of Taiwan (Republic of China).

Appendix A. Supplementary data

Supplementary data associated with this article can be found, in the online version, at doi:10.1016/j.talanta.2009.08.034.

References

[1] C.P. McMahon, G. Rocchitta, S.M. Kirwan, S.J. Killoran, P.A. Serra, J.P. Lowry, R.D. O'Neill, Biosens. Bioelectron. 22 (2007) 1466.
[2] H.A. Al Attar, A.P. Monkman, J. Phys. Chem. B 111 (2007) 12418.
[3] K. Pu, B. Liu, Biosens. Bioelectron. 24 (2009) 1067.
[4] I. Becerik, F. Kadirgan, Synth. Met. 124 (2001) 379.
[5] T. Selvaraju, R.R. Ramaraj, J. Electroanal. Chem. 585 (2005) 290.
[6] M. Mao, D. Zhang, T. Sotomura, K. Nakatsu, N. Koshiba, T. Ohsaka, Electrochim. Acta 48 (2003) 1015.
[7] M. Yasuzawa, A. Kunugi, Electrochem. Commun. 1 (1999) 459.
[8] C.P. Andrieux, O. Haas, J.M. SavGant, J. Am. Chem. Soc. 108 (1986) 8175.
[9] J. Wang, M. Musameh, Anal. Chim. Acta 511 (2004) 33.
[10] H. Cai, X. Cao, Y. Jiang, P. He, Y. Fang, Anal. Bioanal. Chem. 375 (2003) 287.
[11] A. Erdem, P. Papakonstantinou, H. Murphy, Anal. Chem. 78 (2006) 6656.
[12] H. Beitollahi, M.M. Ardakani, H. Naeimi, B. Ganjipour, J. Solid State Electrochem. 13 (2009) 353.
[13] Q. Li, J. Zhang, H. Yan, M. He, Z. Liu, Carbon 42 (2004) 287.
[14] J. Zhang, J.K. Lee, Y. Wu, R.W. Murray, Nano Lett. 3 (2003) 403.
[15] C. Deng, J. Chen, M. Wang, C. Xiao, Z. Nie, S. Yao, Biosens. Bioelectron. 24 (2009) 2091.
[16] R.J. Chen, Y. Zhang, D. Wang, H. Dai, J. Am. Chem. Soc. 123 (2001) 3838.
[17] A.A. Karyakin, E.E. Karyakina, H.L. Schmidt, Electroanalysis 11 (1999) 149.
[18] A.G. MacDiarmid, J.C. Chiang, A.G. Richter, A. Epstein, Synth. Met. 18 (1987) 285.
[19] R. Mazeikiene, G. Niaura, O. Eicher-Lorka, A. Malinauskas, Vib. Spectrosc. 47 (2008) 105.
[20] Q. Wan, X. Wang, X. Wang, N. Yang, Polymer 47 (2006) 7684.
[21] X. Wang, N. Yang, Q. Wan, X. Wang, Sens. Actuators B 128 (2007) 83.
[22] H. Zhao, S. Bennici, J. Shen, A. Auroux, J. Mol. Catal. A: Chem. 309 (2009) 28.
[23] R. Irie, T. Katsuki, Chem. Rec. 4 (2004) 96.
[24] T. Mallat, A. Baiker, Chem. Rev. 104 (2004) 3037.
[25] M.J. Schultz, M.S. Sigman, Tetrahedron 62 (2006) 8227.
[26] A. Bauer, E.L. Gyenge, C.W. Oloman, J. Power Sources 167 (2007) 281.
[27] L.M. Huang, T.C. Wen, J. Power Sources 182 (2008) 32.
[28] S. Engelhard, H.G. Lohmannsroben, F. Schael, Appl. Spectrosc. 58 (2004) 1205.
[29] M. Rocchia, A.M. Rossi, G. Zeppa, Sens. Actuators B 123 (2007) 89.
[30] N.G. Patel, S. Meier, K. Cammann, G.C. Cheminitius, Sens. Actuators B: Chem. 75 (2001) 101.
[31] S.S. Stahl, Angew. Chem. Int. Ed. 43 (2004) 3400.
[32] E. Segal, R. Tchoudakov, M. Narkis, A. Siegmann, Y. Wei, Sens. Actuators B 104 (2005) 140.
[33] E. Akyilmaz, E. Dinckaya, Talanta 53 (2000) 505.
[34] M. Revenga-Parra, T. Garcia, E. Lorenzo, F. Pariente, Sens. Actuators B 130 (2008) 730.
[35] A.G.V. de Prada, N. Pena, C. Parrado, A.J. Reviejo, J.M. Pingarron, Talanta 62 (2004) 896.
[36] N. Darsono, D. Yoon, J. Kim, Appl. Surf. Sci. 254 (2008) 3412.
[37] J. Chen, A.M. Rao, S. Lyuksyutov, M.E. Itkis, R.E. Smalley, R.C. Haddon, J. Phys. Chem. B 105 (2001) 2525.
[38] Y.C. Tsai, S.C. Li, J.M. Chen, Langmuir 21 (2005) 3653.
[39] G.A. Rivas, S.A. Miscoria, J. Desbrieres, G.D. Barrera, Talanta 71 (2007) 270.
[40] S.M. Chen, M.I. Liu, Electrochim. Acta 51 (2006) 4744.
[41] S.M. Chen, C.J. Liao, V.S. Vasantha, J. Electroanal. Chem. 589 (2006) 15.
[42] E. Laviron, J. Electroanal. Chem. 101 (1979) 19.
[43] A. Mohadesi, M.A. Taher, Sens. Actuators B: Chem. 123 (2007) 733.
[44] J. Wang, T. Dai, Yarlagadda, Langmuir 21 (2005) 9.